Green Phosphorescence and Electroluminescence of Sulfur Pentafluoride-Functionalized Cationic Iridium(III) Complexes

Nail M. Shavaleev,[a] Guohua Xie,[b] Shinto Varghese,[b] David B. Cordes,[c] Alexandra M. Z. Slawin,[c] Cristina Momblona,[d] Enrique Ortí,[d] Henk J. Bolink,[d] Ifor D.W. Samuel,[b] and Eli Zysman-Colman[a]**

[a] Organic Semiconductor Centre, EaStCHEM School of Chemistry, University of St Andrews, St Andrews, Fife, UK, KY16 9ST, Fax: +44-1334 463808; Tel: +44-1334 463826; E-mail: eli.zysman-colman@st-andrews.ac.uk; URL: http://www.zysman-colman.com
[b] Organic Semiconductor Centre, SUPA School of Physics and Astronomy, University of St Andrews, North Haugh, St Andrews Fife, KY16 9SS, UK; E-mail: idws@st-andrews.ac.uk
[c] EaStCHEM School of Chemistry, University of St Andrews, St Andrews, Fife, UK, KY16 9ST, Tel: +44-1334 464808; Fax: +44-1334 463808
[d] Instituto de Ciencia Molecular, Universidad de Valencia, C/J. Beltran 2, 46980 Paterna, Spain

ABSTRACT

We report four cationic iridium(III) complexes $[Ir(C^N)_2(dtBubpy)](PF_6)$ that have sulfur-pentafluoride-modified 1-phenylpyrazole and 2-phenylpyridine cyclometalating (C^N) ligands (d*t*Bubpy = 4,4'-di-*tert*-butyl-2,2'-bipyridyl). Three of the complexes were characterized by single-crystal X-ray structure analysis. In cyclic voltammetry, the complexes undergo reversible oxidation of iridium(III) and irreversible reduction of the SF_5 group. They emit bright green

phosphorescence in acetonitrile solution and in thin films at room temperature, with emission maxima between 482–519 nm and photoluminescence quantum yields of up to 79%. The electron-withdrawing sulfur pentafluoride group on the cyclometalating ligands increases the oxidation potential and the redox gap and blue-shifts the phosphorescence of the iridium complexes more than do the commonly-employed fluoro and trifluoromethyl groups. The irreversible reduction of the SF_5 group may be a problem in organic electronics; for example, the complexes do not exhibit electroluminescence in light-emitting electrochemical cells (LEECs). Nevertheless, the complexes exhibit green to yellow-green electroluminescence in doped multi-layer organic light-emitting diodes (OLEDs) with emission maxima ranging from 501–520 nm and with an external quantum efficiency (EQE) of up to 1.7% in solution-processed devices.

Introduction.

One particular class of emitters that has been widely studied in electroluminescent (EL) devices is phosphorescent cyclometalated iridium(III) complexes.[1] Iridium complexes are attractive as their frequently bright emission can be tuned across the visible spectrum through simple ligand modification.[2] Blue emitters are required for color displays and to generate white light for lighting applications.[3] Two strategies can be adopted to blue-shift the phosphorescence of a cyclometalated Ir(III) complex: the first is to increase the energy of the emissive metal-to-ligand, intra-ligand or ligand-to-ligand charge-transfer (MLCT, ILCT and LLCT, respectively) excited states by introducing electron-donating/-withdrawing groups to the ligands and by disrupting communication between the ligands;[2b-d,4] the second way is to increase the energy of the emissive π–π^* ligand-centered states by limiting conjugation in the ligand.[2b-d,5] The frequently used electron-withdrawing groups on the cyclometaling ligand (C^N) that blue-shift

the phosphorescence of Ir(III) complexes are fluoro,[6] trifluoromethyl,[6a,6b,7] sulfonyl,[8] and cyclometalated heterocycles such as 2,3'-bipyridinato.[9]

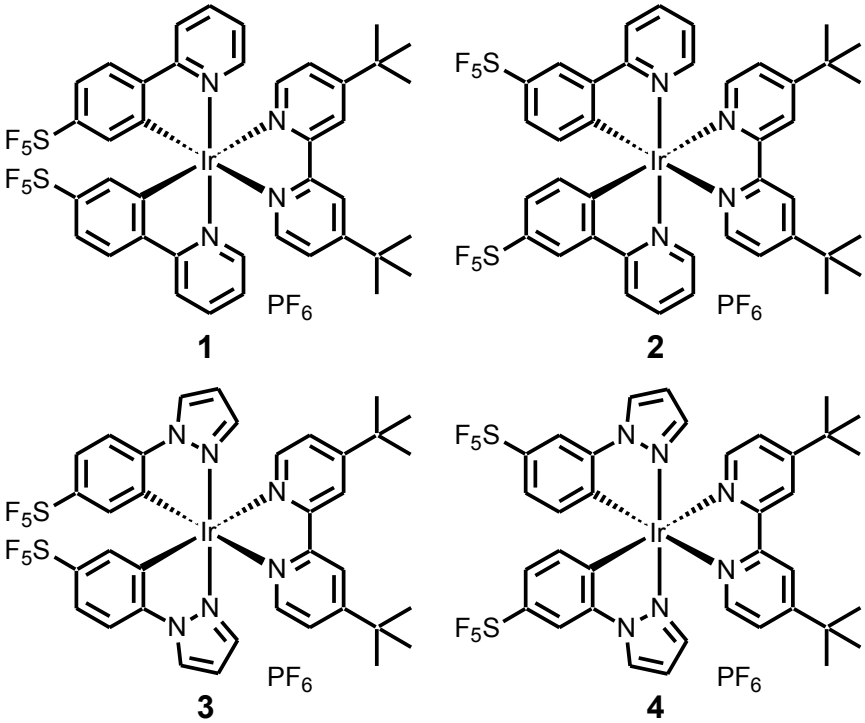

Chart **1**. New complexes.

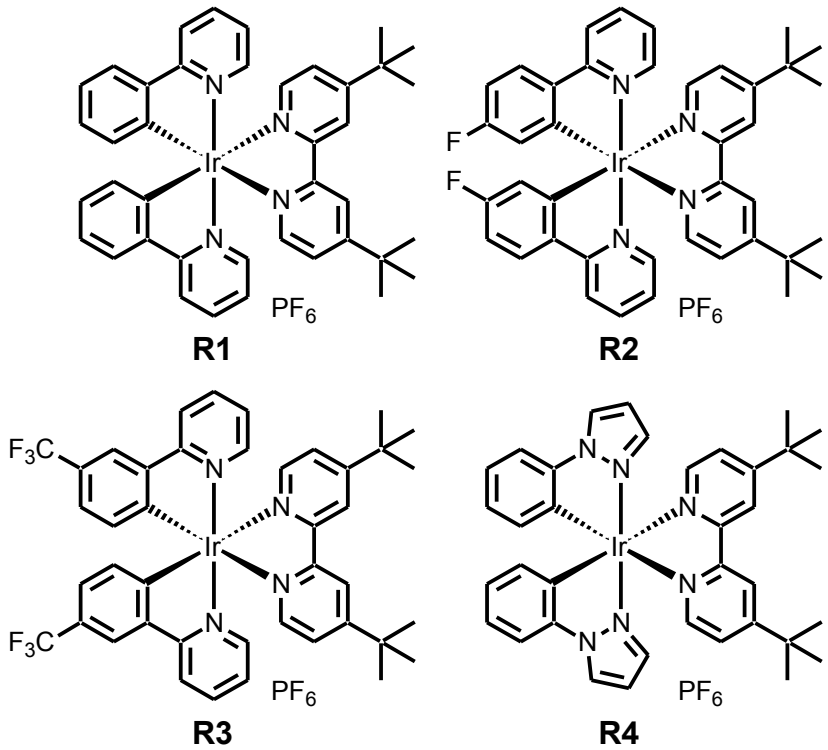

Chart **2**. Reference complexes.

Organic sulfur pentafluoride compounds have been known for the past 50 years and they have been used in materials and medicinal chemistry.[10] Metal complexes that have sulfur pentafluoride groups (SF_5) are, however, rare.[11] It is surprising that this group has received such little attention especially considering that SF_5 is a bulky, chemically inert, polar, hydrophobic and very strong electron-withdrawing group.[10c,12] Notably, it is less-reactive and more electron-withdrawing than the CF_3 group, making it a potentially desirable alternative moiety for optoelectronic tuning strategies.[10c,13]

Here, we describe four cyclometalated iridium(III) complexes, **1**–**4**, that have a sulfur pentafluoride group (Chart **1**). We investigate the effect of the SF_5 group on their phosphorescence and electrochemistry and study their electroluminescence in two-layer light-

emitting electrochemical cells (LEECs) and in doped multi-layer organic light emitting diodes (OLEDs). We compare these complexes to their non-substituted and fluoro- and trifluoromethyl-substituted analogues **R1**–**R4** (Chart **2**).[6d,6f,6g,14]

Results and Discussion.

Synthesis.

Four new cyclometalating ligands **L1**–**L4** were prepared (Scheme **1**). **L1** and **L2** were obtained by Stille[15] coupling of commercially available 3- or 4-bromophenylsulfur pentafluorides with 2-(tri-*n*-butylstannyl)pyridine in 81% and 72% yield, respectively. The tin by-products were removed by passing the reaction mixture through silica gel and (10% by weight) potassium carbonate.[16] **L3** was obtained by a non-catalysed C–N coupling of electron-deficient 4-bromophenylsulfur pentafluoride with pyrazole in the presence of potassium *tert*-butoxide in DMSO in 53% yield.[17] In contrast, the reaction of 3-bromophenylsulfur pentafluoride with pyrazole to make **L4** under the same conditions gave a mixture of products. Therefore, **L4** was prepared from a Cu_2O catalyzed C–N coupling of these two reagents in DMF in the presence of cesium carbonate in 77% yield.[18] The successful syntheses of **L3** and **L4** confirm that the SF_5 group is stable to strong bases at high temperatures in organic solvents. The 4-SF_5 ligands **L1** and **L3** are white solids while the 3-SF_5 ligands **L2** and **L4** are colorless oils.

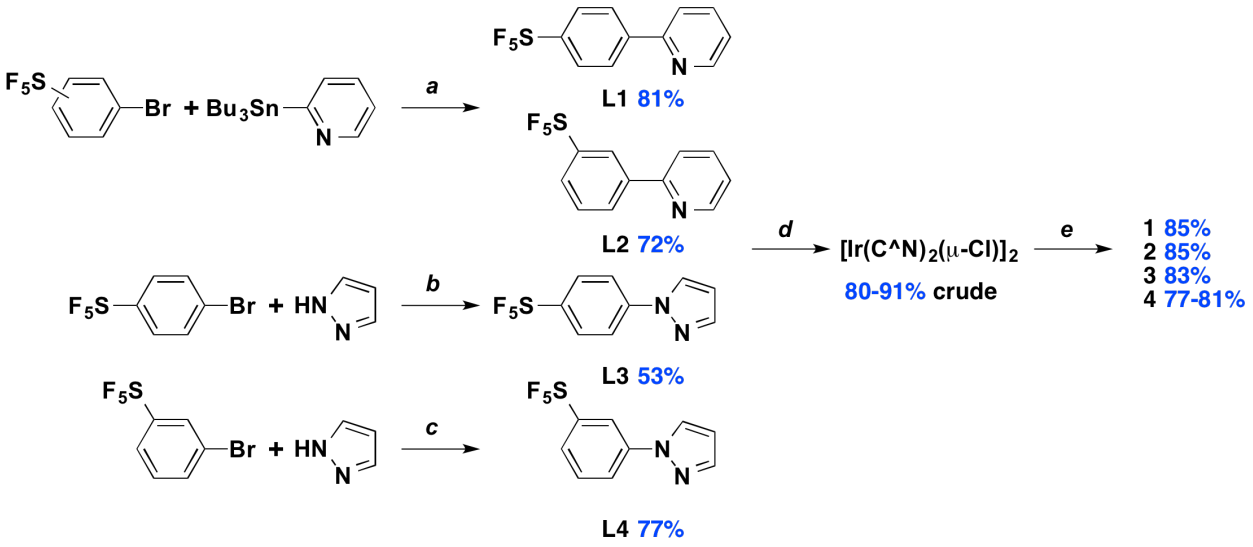

Scheme **1**. Synthesis of **L1**–**L4** and **1**–**4**. (a) $[Pd(PPh_3)_4]$ (catalyst), toluene, under N_2, 120 °C; (b) KO*t*Bu, DMSO, under N_2, 140 °C; (c) Cs_2CO_3, Cu_2O (catalyst), DMF, under N_2, 120 °C; (d) C^N ligand **L1**–**L4**, 2-ethoxyethanol/water, $IrCl_3 \cdot 3H_2O$, under N_2, 120 °C; (e) (i) 4,4'-di-*tert*-butyl-2,2'-bipyridine, dichloromethane/methanol, under N_2, 40 °C; (ii) NH_4PF_6, methanol/water, under air, room temperature.

The reaction of ligands **L1**–**L4** with $IrCl_3 \cdot 3H_2O$ in 2-ethoxyethanol/water gave the dinuclear Ir(III) complexes $[Ir(C^N)_2(\mu\text{-}Cl)]_2$ as yellow solids in 80–91% yield, which were used without purification.[19] These iridium dimers were cleaved with 4,4'-di-*tert*-butyl-2,2'-bipyridyl (d*t*Bubpy) in dichloromethane/methanol to afford the target cationic complexes $[Ir(C^N)_2(dtBubpy)](PF_6)$, **1**–**4**, in 77–85% yield as their hexafluorophosphate salts after purification by column chromatography and the anion exchange (Scheme **1**). The complexes **1**–**4** are air- and moisture-stable solids that are soluble in polar organic solvents.

New compounds were characterized by elemental analysis, ^1H and ^{19}F NMR spectroscopy, mass-spectrometry, and single crystal X-ray structure analysis. The ^{19}F NMR

spectra exhibit the characteristic signals of the SF_5 group: a 'pentet' for the axial fluorine and a 'doublet' for the equatorial fluorines in a 1-to-4 intensity ratio (the fluorines in the SF_5 group behave as an AB_4 system in the ^{19}F NMR experiment).[20] The NMR spectra confirm that the complexes **1**–**4** have C_2-symmetry. The mass-spectra of **1**–**4** exhibit the characteristic peak of the cation $[Ir(C^N)_2(dtBubpy]^+$.

The characterization of the complexes **1**–**3** confirms that they are pure. In contrast, complex **4** contains a trace impurity: it is observed in the ^1H NMR and it could not be removed by a combination of chromatography and recrystallization. In light of the satisfactory microanalysis for this complex, we consider that this impurity is an isomer, in which one of the SF_5 groups is not in the *para*- but in the *ortho*-position to Ir(III). In fact, the formation of *para*- and *ortho*-isomers of Ir(III) complexes was observed previously for some of the C^N ligands with a 3-substituent in the phenyl ring.[21] Small-scale recrystallization of **4** provided single crystals that by X-ray analysis confirmed the presence of the expected *para*-isomer (Figure **1**).

The incorporation of the electron-withdrawing SF_5 group onto the scaffold of the C^N ligand is designed to increase the energy of charge-transfer excited states of the Ir(III) complexes. We prepared both a pyridine and pyrazole series of C^N ligands and complexes. Replacing pyridine by pyrazole has been previously shown to blue-shift the emission of Ir(III) complexes[6d,22] as pyrazole has higher-energy π–π^* states and it is both a weaker σ- and π-donor to metal ions than pyridine.[23] We chose d*t*Bubpy to improve solubility of the complexes and to compare them with the references **R1**–**R4** (Chart **2**).[6d,6f,6g,14]

Crystal Structures.

Figure **1** and Table **1** report the X-ray structures of **1**, **3**, and **4**. In each case the, Ir(III) ion exhibits a distorted octahedral coordination environment with the two N atoms of the C^N ligands *trans* to each other. The Ir–C and Ir–N bond lengths are similar for the 1-arylpyrazole ligands in the [Ir–(C^N)] fragment in **3** and **4** [2.015(3)–2.025(3) Å for Ir–C_{C^N}; 2.014(2)–2.029(4) Å for Ir–N_{C^N}]. In contrast, for the 2-arylpyridine ligands in **1**, the Ir–N_{C^N} bond, 2.051(4) and 2.055(4) Å, is longer than the Ir–C_{C^N} bond, 2.016(4) and 2.021(6) Å. The Ir–N bond to the ancillary d*t*Bubpy ligand, 2.116(2)–2.135(2) Å, is longer than that to the C^N ligands, 2.014(2)–2.055(4) Å. The 1-arylpyrazoles in **3** and **4** are more planar [dihedral angles of 3.79(9)–6.18(11)°] than the 2-arylpyridines in **1** [5.2(3) and 13.5(4)°]. The sulfur atom of the aryl–SF_5 group is in an octahedral environment and possesses similar axial and equatorial S–F bond lengths. The equatorial S–F bonds are out of the plane of the aryl ring. The bulky SF_5 and *tert*-butyl groups prevent face-to-face π–π stacking of the complexes. The minimum Ir···Ir distance exceeds 9 Å.

Table 1. Structural Parameters[a]

	Bond lengths (Å)			Dihedral Angles (°)[b]		
	C^N		d*t*Bubpy			Ir···Ir (Å)[d]
Complex	Ir–C	Ir–N_{C^N}	Ir–N_{N^N}[c]	C^N	N^N	
1	2.016(4)	2.051(4)	2.133(3)	5.2(3)	4.7(2)	9.0142(8)
	2.021(6)	2.055(4)	2.116(5)	13.5(4)		
3	2.017(4)	2.029(4)	2.119(4)	4.90(11)	8.24(9)	9.0144(6)
	2.022(4)	2.015(4)	2.118(4)	5.45(19)		
4	2.015(3)	2.025(2)	2.135(2)	3.79(9)	8.31(10)	9.8946
	2.025(3)	2.014(2)	2.116(2)	6.18(11)		

[a] Each row corresponds to one C^N ligand in the complex. [b] The dihedral angle between the rings of the ligands. [c] N-atom of the d*t*Bubpy ligand is *trans* to the C-atom of the C^N ligand in the same row. [d] Minimum Ir···Ir distance.

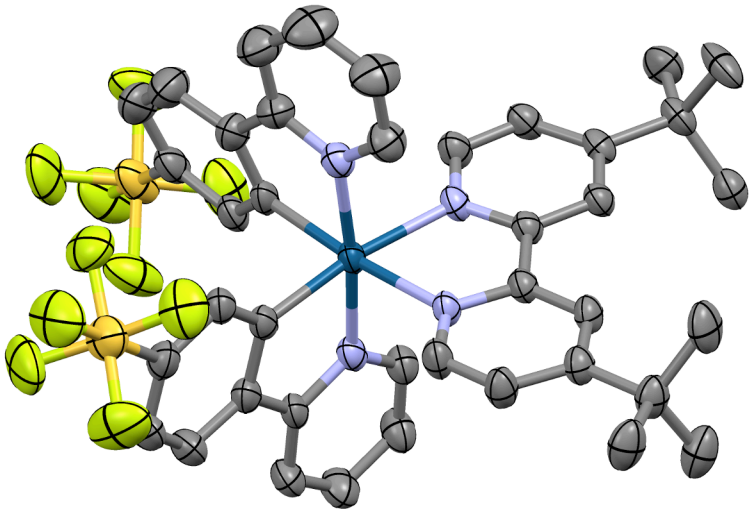

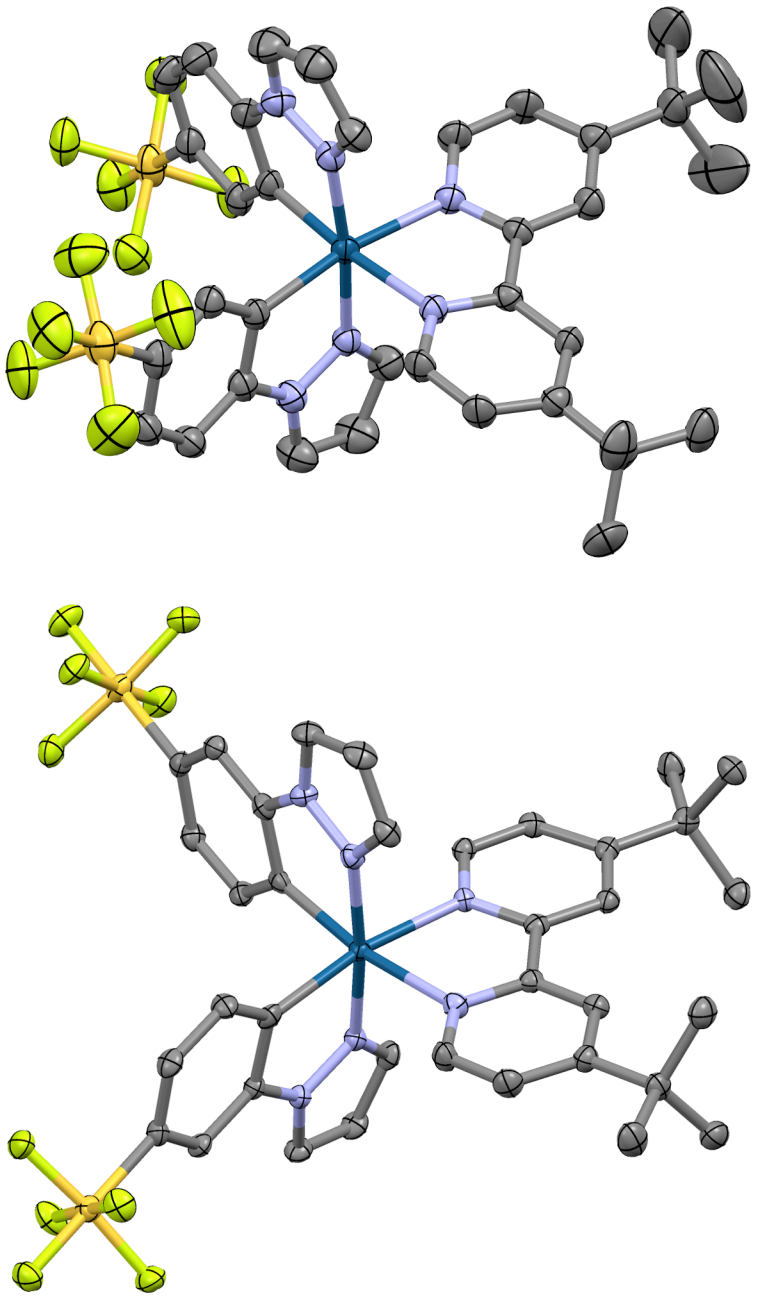

Figure **1.** Structures of complexes **1**, **3**, and **4** (50% probability ellipsoids; H atoms, PF_6 anion, and co-crystallized solvent molecules omitted). Heteroatoms: N, light blue; F, green; S, orange; and Ir, dark blue.

Electrochemistry.

The redox properties of the complexes were studied by cyclic voltammetry, CV, (Figure **2** and Table **2**). The oxidation potential of **1**–**4** in DMF is beyond the electrochemical window of the solvent. In acetonitrile, **1**–**4** exhibit a reversible oxidation of iridium(III) at 1.19–1.29 V (at scan rate of 0.1 V s^{-1}; referenced against the ferrocene couple). Its potential increases by 70–90 mV when pyridine is replaced with pyrazole, which is a weaker electron donor,[23] and by 10–30 mV when the SF_5 group is moved from *meta*- to *para* with respect to the Ir–C bond of the C^N ligand.

Table **2**. Electrochemistry[a]

Complex	$E^{ox}_{1/2}$ /V (ΔE_p /mV)	$E^{red}_{1/2}$ /V (ΔE_p /mV)	ΔE /V [b]
1	1.19 (68)		
2	1.20 (68)		
3	1.26 (75)		
4	1.29 (70)	−1.83 (100)[c]	3.12
R1[14a]	0.83	−1.88	2.71
R2[6g]	1.02	−1.84	2.86
R3[14b]	1.13	−1.82	2.95
R4[6d]	0.95	−1.89	2.84

[a] In MeCN with 0.1 M (nBu$_4$N)PF_6 on glassy-carbon (GC) working electrode, platinum spiral counter electrode and platinum wire quasi-reference electrode at a scan rate of 0.1 V s^{-1}, unless stated otherwise. $E^{ox}_{1/2}$ are reported relative to Fc^+/Fc. The peak separation, ΔE_p for **1**–**4** is given in brackets (for the Fc^+/Fc it was 60–63 mV). The reduction is a sequence of irreversible processes and its (onset of) potential depends on the scan rate. Error: ±30 mV. Redox potentials of **1**–**4** at 1 V s^{-1} are given in Table S2. [b] $\Delta E = E^{ox}_{1/2} - E^{red}_{1/2}$. [c] Data reported at scan rate of 1 V s^{-1} (irreversible for **1**–**3**).

Complexes **1**–**4** exhibit a cascade of irreversible reduction processes in MeCN and in DMF with an onset at −1.6 V to −1.8 V (Figure **2** and Figure **S1** and **S2** in the Supporting Information). These reductions likely involve the electron-deficient SF_5 group and, for **2** and **4**, the d*t*Bubpy ligand. The SF_5 group on accepting an electron may release a fluoride, thereby making the reduction irreversible.[10a] At the faster scan of 1 V s^{-1}, the first reduction of **2** and **4** resembles a one-electron process, and in the case of **4** it becomes quasi-reversible at −1.83 V, a typical reduction potential for d*t*Bubpy in $[Ir(C^N)_2(dtBubpy)]^+$ complexes (Table **S2** and Figure **S2**).[6f,6g,14b]

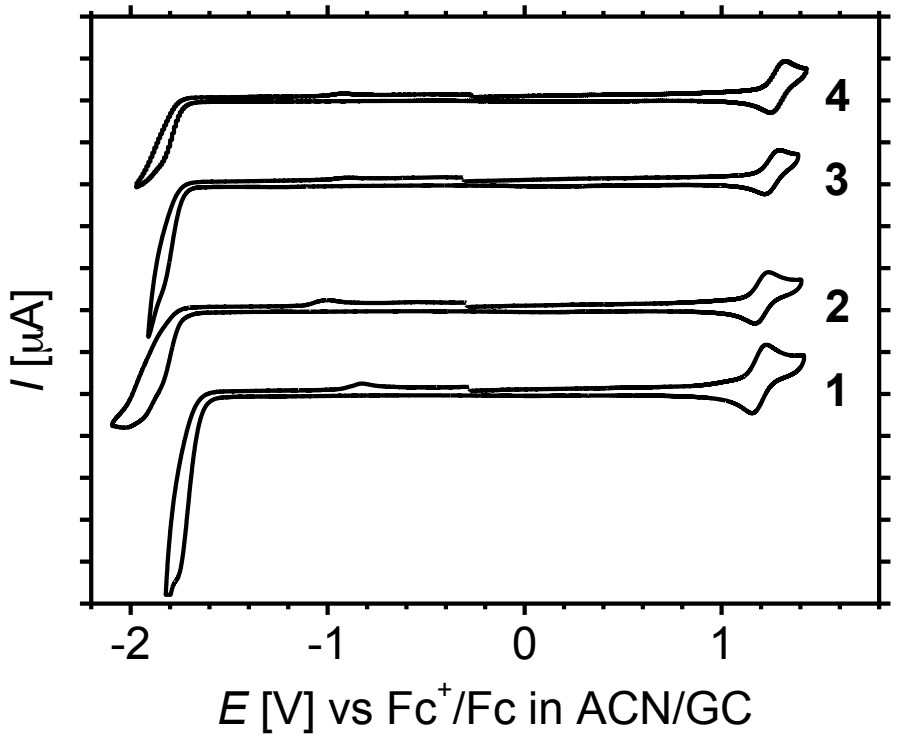

Figure **2.** Cyclic voltammograms of **1**–**4** in MeCN (glassy-carbon electrode, 0.1 M nBu_4NPF_6, 0.1 V s^{-1}; clockwise scan). The unit on the vertical axis is 10 μA. The peaks at −1.2 V to −0.2 V

in the CVs are the return waves of the irreversible reduction. CVs of **1–4** at 1 V s^{-1} are shown in Figure **S2**.

The ligands **L1–L4** also exhibit irreversible reduction waves with peak potential at −2.17 V to −2.59 V at scan rate of 0.1 V s^{-1} (Table **S3** and Figures **S3** and **S4**). Their reduction potential is more positive than that of the reference ligand 2-phenylpyridine, ppyH , of −2.79 V at 1 V s^{-1}. The reduction of ppyH is quasi-reversible at 1 V s^{-1}, but irreversible at slower scan rates (Figure **S3** and Table **S3**). The onsets and peaks of the reduction potentials of the SF_5-compounds **1–4** and **L1–L4** depend on the scan rate and on the solvent and, therefore, are not discussed.

Comparison of **1–4** with the reference complexes **R1–R4** demonstrates that the SF_5 group positively shifts the oxidation potential of the complex by 360 mV and 370 mV from **R1** (non-substituted analogs) to **1** and **2**, respectively; by 310 mV and 340 mV from **R4** (non-substituted analog) to **3** and **4**, respectively; by 170 mV from **R2** (F-analog) to **1**; and by 70 mV from **R3** (CF_3-analog) to **2** (Table **2**). In contrast to the irreversible multi-electron reduction of **1–4**, the references **R1–R4** exhibit a reversible one-electron reduction of d*t*Bubpy at −1.89 V to −1.82 V (Table **2**). The redox gap, $\Delta E = E^{ox}_{1/2} - E^{red}_{1/2}$, increases by 170–410 mV from **R1–R4** to the SF_5-complex **4**.

Absorption and Emission Spectroscopy.

The complexes **1–4** are pale yellow to yellow solids. The absorption spectra of **1–4** in MeCN solution do not exhibit well-resolved bands (Figure **3**). However, they do show intense

$\pi \rightarrow \pi^*$ transitions in the UV range with molar absorption coefficients (ε) of $>10^4$ M^{-1} cm^{-1} (Figure **3** and Table **S4**). The weaker-intensity (ε $<10^4$ M^{-1} cm^{-1}) lower-energy mixed charge-transfer transitions tail from the UV to 420–490 nm in the visible range.[2b,24]

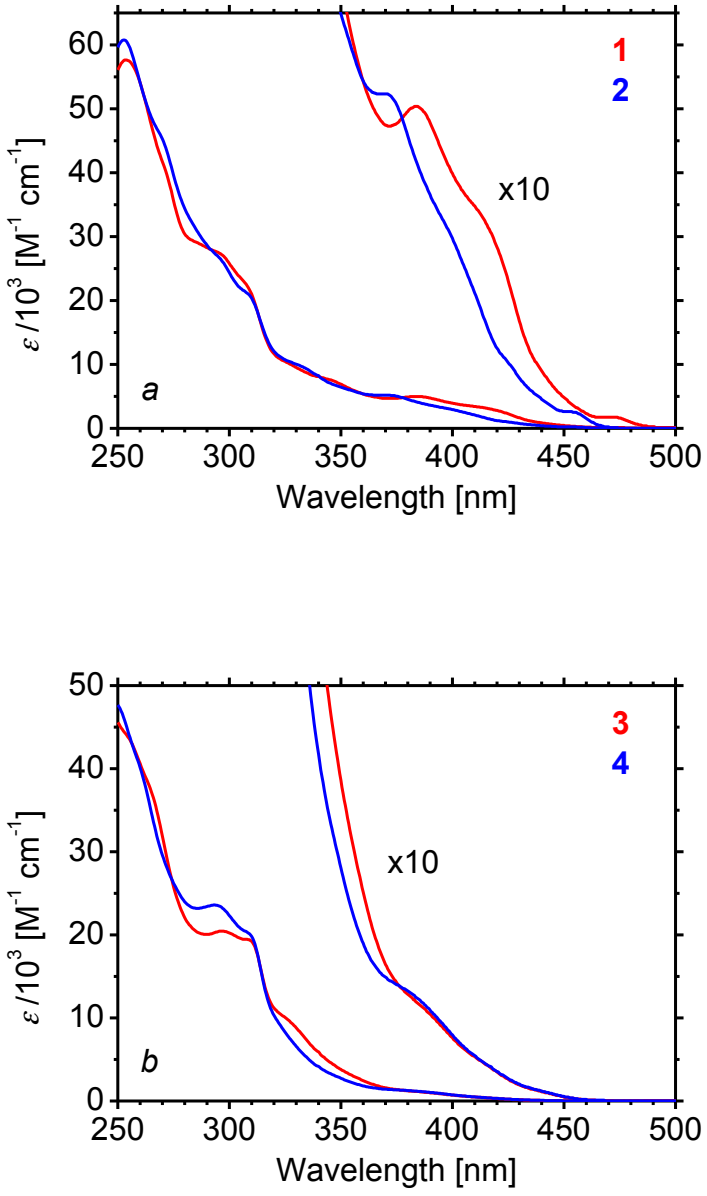

Figure **3.** Absorption spectra of complexes in MeCN: (a) **1** and **2**; (b) **3** and **4**.

In the solid state and in MeCN solution at room temperature **1**–**4** exhibit green luminescence. The emission intensity increases on removing oxygen from the solutions, a hallmark of phosphorescence. In degassed dilute MeCN solution, **1** and **2** exhibit structured emission while the emission of **3** and **4** is broad and unstructured (Figure **4**). We note that the absorption transitions at >350 nm are likewise more structured for **1** and **2** and are broader for **3** and **4** (Figure **3**).

The photophysical behavior of **1**–**4** is summarized in Table **3** and the emission spectra are shown in Figure **4**. All complexes are bright emitters with high photoluminescence quantum yields (Φ_{PL}) ranging from 70–79%. The observed emission lifetimes (τ_e) are mono-exponential, indicating the presence of a single emissive species (cf. Figure **S6**) and are on the microsecond timescale (1.4–4.7 μs). The calculated radiative lifetimes, $\tau_{rad} = \tau_e \times \Phi_{PL}^{-1}$, are 2.0–6.0 μs, and are typical of phosphorescence from a mixed metal-to-ligand charge transfer (MLCT) and ligand-to-ligand charge transfer (LLCT) excited state.[2b,24] In dichloromethane (DCM) solution (when compared to MeCN), the emission profiles do not change for **1**, broaden for **2**, and become more structured for **3** and **4**, with an observed blue-shift of up to 8 nm (Figure **4**).

Table **3**. Photophysical data[a]

	Medium	λ_{0-0} (nm)	λ_{0-1} (nm)	λ_{max} (nm)	Φ_{PL} (%)	τ_e (μs)	τ_{rad} (μs)
1	MeCN	482	517	482	79	4.7	6.0
	DCM	482	514	482			
	Film	491	519	519	19		
2	MeCN	465	496	496	71	2.0	2.8
	DCM			498			
	Film			507	48		
3	MeCN			505	71	1.4	2.0
	DCM			497			
	Film			494	69		
4	MeCN			500	70	1.5	2.1
	DCM			494			
	Film			493	74		
R1[14a]	MeCN			581			
R2[6g]	MeCN			552			
R3[14b]	DCM			512			
R4[6d]	MeCN			555			

[a] In degassed MeCN or DCM solution. In spin-coated thin film of **1**–**4** and [BMIM][PF_6] in a 4-to-1 molar ratio under air at room temperature. The 0–0 and 0–1 transitions for the structured spectra and the emission maximum are given.

The presence of the vibronic structure in both the phosphorescence and the low-energy absorption spectra and the relatively longer radiative lifetimes of the pyridine complexes **1** and **2** suggest an emission from an excited state of mixed ligand-centered (involving the C^N ligand)

and charge-transfer character.[4] The variation of the regiochemistry of the SF_5 group from *meta* (**1**) to *para* (**2**) to Ir–C bond blue-shifts both the absorption and the emission spectra and changes the photophysics of **1** and **2**, probably because their emissive state involves the C^N ligands. The ligand-centered character of the emissive state is likely more pronounced in **1** than in **2**, because **1** exhibits a solvent-independent phosphorescence spectrum and the longest radiative lifetime.[2b]

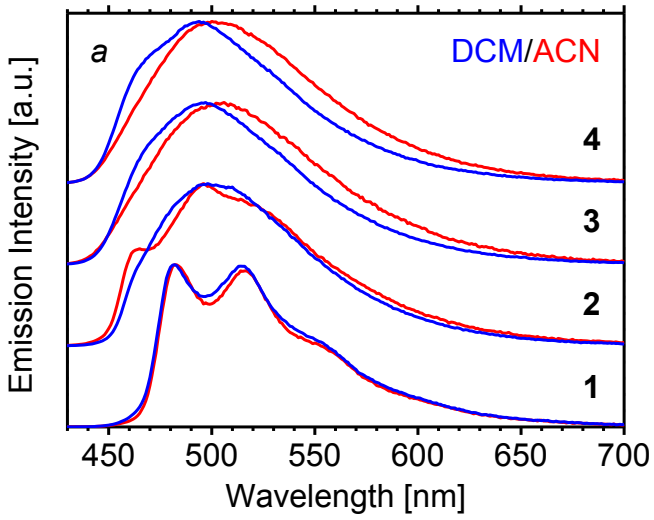

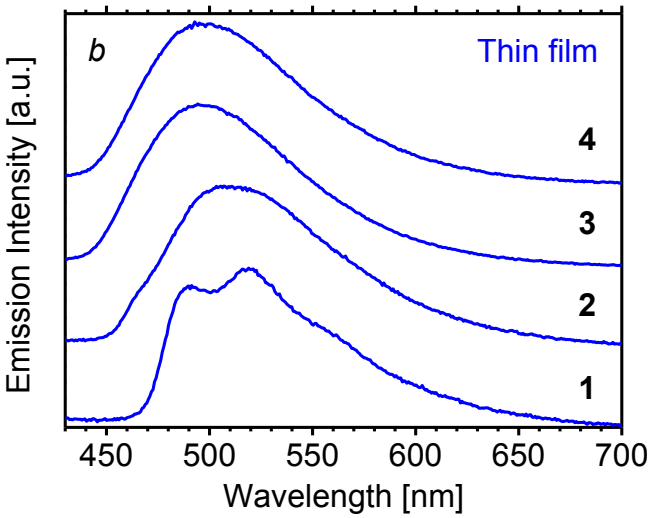

Figure **4.** Phosphorescence spectra of **1**–**4.** (a) in MeCN and in DCM (room temperature; λ_{exc} = 360 nm; $\Delta\lambda_{em}$ = 2 nm) under nitrogen; (b) in thin films of **1**–**4** and the ionic liquid [BMIM][PF_6] in a 4-to-1 molar ratio under air.

The excited states of the cyclometalating ligands shift to higher energy when pyridine is replaced by pyrazole (Figure **S5**).[6d] Indeed, the broad and solvent-sensitive phosphorescence spectra and the shorter radiative lifetimes of the pyrazole-containing complexes **3** and **4** suggest a predominantly charge-transfer emissive state.[2b,24] Unlike **1** and **2**, the position of the SF_5 group does not influence the spectroscopic properties of **3** and **4**, because their emissive state is localized predominantly on the [Ir–(d*t*Bubpy)] fragment.

In thin films of **1**–**4** doped with the ionic liquid (IL) 1-*n*-butyl-3-methylimidazolium hexafluorophosphate [BMIM][PF_6] in a 4-to-1 molar ratio under air, the complexes exhibit phosphorescence behavior similar to that in solution and with Φ_{PL} of 19–74% (cf. Figure **4**). These observations, coupled with the solid-state X-ray structures (Figure **1**), confirm that bulky SF_5 and *tert*-butyl groups prevent intermolecular interaction of **1**–**4**.

The onset of the phosphorescence spectrum blue-shifts when pyridine (**1** and **2**) is replaced by pyrazole (**3** and **4**) (Figure **4b**). The blue-shifts in the absorption cut-off and in the λ_{0-0}, λ_{max}, and onset of the phosphorescence spectra of **1**–**4** qualitatively match the increase in their oxidation potentials (Tables **2** and **3**). The phosphorescence maximum of **1**–**4** in solution at 482–505 nm is significantly blue-shifted when compared to that of the references **R1**–**R4** at 512–581 nm (Table 3).

Electroluminescence: Light-Emitting Electrochemical Cells.

The electroluminescence (EL) of **1**–**4** was tested in light-emitting electrochemical cells (LEEC). The architecture of the devices was ITO/PEDOT:PSS (80 nm)/(**1**–**4**):[BMIM][PF_6] (4-to-1; 150 nm)/Al (70 nm), where PEDOT:PSS is poly(3,4-ethylenedioxythiophene):poly-styrenesulfonate. The active layer was made of the emitters **1**–**4** and [BMIM][PF_6] in a 4-to-1 molar ratio. The ionic liquid increases the concentration of ionic species and the ionic mobility,[25] thereby reducing the turn-on time of the LEEC. The LEECs were driven with a pulsed current at a block wave frequency of 1000 Hz, and a duty cycle of 50%. The current density of the pulse was 100 or 200 A m^{-2}; the average current density was 50 or 100 A m^{-2}, respectively. The pulsed-current driving was chosen because it rapidly injects the charges, lowers turn-on time, stabilizes the growing of the intrinsic doped regions, and increases lifetime of the device.[26]

Although **1**–**4** emit efficient photoluminescence in films (Table **3** and Figure **4**), they do not exhibit electroluminescence in the LEEC. Initially, charges are injected into the LEEC and the injection barrier is lowered;[27] however, the voltage significantly increases after a maximum of 10 h and the current stops, indicating problems with charge-injection (Figure **S7**). In order for LEECs to function the complex must be able to serve as a charge carrier, and to do that it must undergo redox processes without chemical decomposition.[1c,1d] We consider that the lack of electroluminescence of **1**–**4** in the LEECs arises from the electrochemical instability of the SF_5 group.

Electroluminescence: Organic Light-Emitting Diodes.

The electroluminescence of the complexes was evaluated in doped multi-layer organic light-emitting diodes (OLEDs). We note that charged emitters are not frequently applied in OLEDs.[28] The device architecture was ITO/PEDOT:PSS (30 nm)/PVK (30 nm)/mCP:OXD-7:complex (74:20:6; 20 nm)/B3PYMPM (50 nm)/Ca (20 nm)/Al (100 nm). PEDOT:PSS acts as a hole-injecting layer; poly(*N*-vinylcarbazole) (PVK), is a hole-transporting and electron/exciton-blocking layer (LUMO = 2.2 eV); 3,5′-*N*,*N*′-dicarbazole-benzene (mCP; triplet level, E_T = 2.9 eV) and 1,3-bis[(4-*tert*-butylphenyl)-1,3,4-oxadiazolyl]phenylene (OXD-7; E_T = 2.7 eV) are the hosts;[29] and 4,6-bis(3,5-di(pyridin-3-yl)phenyl)-2-methylpyrimidine (B3PYMPM) is an electron-transporting and hole-blocking layer [electron mobility ~10^{-5} cm^2 $(V\ s)^{-1}$; HOMO = 6.8 eV].[30] The multi-layer architecture helps to balance the hole/electron-injection and confines the excitons in the emitting layer to give a higher device performance.

Table **4**. Electroluminescence[a]

Complex	V_{on} (V)[b]	λ_{max} (nm)[c]	FWHM (nm)[d]	EQE (%)[e]	CE (cd A^{-1})[f]	PE (lm W^{-1})[g]	CIE[h]
1	8.8	520[i]	94	0.2	0.7	0.2	(0.29, 0.54)
2	8.1	501	115	1.7	4.5	1.5	(0.29, 0.48)
3	8.3	504	106	0.4	1.0	0.3	(0.25, 0.44)
4	7.9	511	125	1.1	3.0	1.3	(0.29, 0.46)

[a] OLED: ITO/PEDOT:PSS (30 nm)/PVK (30 nm)/mCP:OXD-7:complex (74:20:6; 20 nm)/B3PYMPM (50 nm)/Ca (20 nm)/Al (100 nm). [b] Turn-on voltage at 1 cd m^{-2}. [c] Peak wavelength at 10 mA cm^{-2}. [d] Full width at half maximum of the EL spectrum at 10 mA cm^{-2}. [e] Maximum external quantum efficiency. [f] Maximum current efficiency. [g] Maximum power efficiency. [h] The Commission Internationale de L'Eclairage coordinates at 10 mA cm^{-2}. [i] The λ_{0-1} transition; the less-intense λ_{0-0} transition is at 488 nm.

OLED performance data is compiled in Table **4** with EL spectra shown in Figure **5**. Complexes **1**–**4** exhibit green to yellow-green electroluminescence with CIE coordinates of (0.25–0.29, 0.44–0.54) and with the turn-on voltage of 7.9–8.8 V (cf. Figures **S8–S10**). The electroluminescence spectra are structured for **1**, less-structured for **2**, and broad for **3** and **4**. The EL spectra exhibit similar profiles to the solution photoluminescence spectra (Figure **4**), except for the change in the relative intensity of the vibronic peaks for **1**. The EL spectra red-shift when the current density is increased (Figure **S8**). This is due in part to the polarization of the emitter at high current density. Similar behavior has been reported previously in both LEEC and OLED devices.[1c,31] The full width at half maximum (FWHM) of the EL spectrum at 10 mA cm^{-2} varies from 94 nm for **1** to 125 nm for **4**.

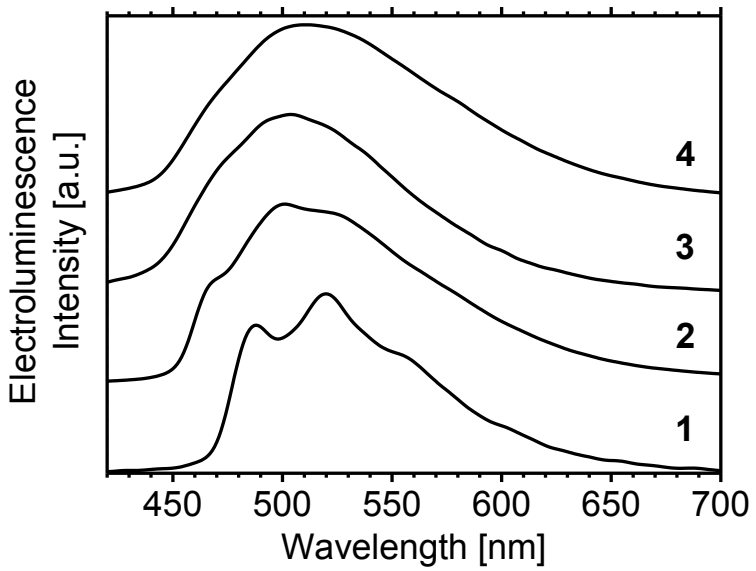

Figure 5. Electroluminescence spectra of complexes **1**–**4** in OLED at 10 mA cm^{-2}.

The devices exhibit similar current densities at low driving voltage of <4 V (Figure **S9**). The OLED with complex **2** at high voltage >7 V exhibits the highest current density but the lowest luminance in the series, indicating unbalanced charge injection. Nevertheless, at low current density, it exhibits the highest current, power, and external quantum efficiencies of 4.5 cd A^{-1}, 1.5 lm W^{-1}, and 1.7% in the series (cf. Figure **S10**). In contrast to LEEC devices, the transport of charges in the doped OLED is mainly performed by the hosts and charge-transporters.[3] Therefore, redox instability of the emitter is less of an issue in OLEDs. It is evidenced by the observation of electroluminescence in the OLED with **1**–**4** acting as the emitters.

Conclusions.

Herein, we report the first examples of iridium complexes bearing the strongly electron-withdrawing sulfur pentafluoride group. Both the ligands and metal complexes are accessible and chemically stable. Complexes **1**–**4** exhibit efficient green phosphorescence under ambient conditions in solution with high Φ_{PL} values, ranging from 70–79%. Sulfur pentafluoride acts as a stronger electron-withdrawing group than fluorine and trifluoromethyl, which is confirmed by blue-shift of the phosphorescence spectra and by the more positive oxidation potentials of the SF_5-modified iridium complexes **1**–**4** compared to the F- and CF_3-analogs **R2** and **R3**. The bulky SF_5 prevents intermolecular interaction of metal complexes in the solid state and increases their solubility; however, its use in organic electronics may be limited by its irreversible reduction, for example, the complexes **1**–**4** exhibit electroluminescence in OLED, but not in LEEC.

Acknowledgements. EZ-C acknowledges the University of St Andrews for financial support. We thank Johnson Matthey and Umicore AG for the gift of materials. We thank the EPSRC UK National Mass Spectrometry Facility at Swansea University for analytical services. EO and CM acknowledge support from the Spanish Ministry of Economy and Competitiveness (MINECO) (CTQ2012-31914), and the Generalitat Valenciana (Prometeo/2012/053). CM would like to thank the MINECO for a predoctoral contract for doctoral training grant (previously FPI).

Supporting Information. Synthesis of ligands and complexes; cyclic voltammetry; absorption, luminescence, and NMR spectra; characterization of LEEC and OLED devices; crystallographic data; CIF of the crystal structures, CCDC 1053870–1053872. This material is available free of charge via the Internet at http://pubs.acs.org.

References

(1) (a) Chi, Y.; Chou, P.-T. *Chem. Soc. Rev.* **2010**, *39*, 638; (b) Zhou, G.; Wong, W. Y.; Yang, X. *Chem. Asian J.* **2011**, *6*, 1706; (c) Hu, T.; He, L.; Duan, L.; Qiu, Y. *J. Mater. Chem.* **2012**, *22*, 4206; (d) Costa, R. D.; Ortí, E.; Bolink, H. J.; Monti, F.; Accorsi, G.; Armaroli, N. *Angew. Chem. Int. Ed.* **2012**, *51*, 8178.
(2) (a) Lowry, M. S.; Bernhard, S. *Chem. Eur. J.* **2006**, *12*, 7970; (b) Flamigni, L.; Barbieri, A.; Sabatini, C.; Ventura, B.; Barigelletti, F. *Top. Curr. Chem.* **2007**, *281*, 143; (c) You, Y.; Park, S. Y. *Dalton Trans.* **2009**, 1267; (d) Ladouceur, S.; Zysman-Colman, E. *Eur. J. Inorg. Chem.* **2013**, *2013*, 2985.
(3) (a) Wen, S.-W.; Lee, M.-T.; Chen, C. H. *J. Display Technol.* **2005**, *1*, 90; (b) Hatwar, T. K.; Kondakova, M. E.; Giesen, D. J.; Spindler, J., P. In *Organic Electronics: Materials, Processing, Devices and Applications*; So, F., Ed.; CRC Press: Boca Raton, Fl, **2009**, 433; (c) Kamtekar, K. T.; Monkman, A. P.; Bryce, M. R. *Adv. Mater.* **2010**, *22*, 572.
(4) Ladouceur, S.; Swanick, K. N.; Gallagher-Duval, S.; Ding, Z.; Zysman-Colman, E. *Eur. J. Inorg. Chem.* **2013**, *2013*, 5329.
(5) (a) Baranoff, E.; Yum, J.-H.; Graetzel, M.; Nazeeruddin, M. K. *J. Organomet. Chem.* **2009**, *694*, 2661; (b) Darmawan, N.; Yang, C. H.; Mauro, M.; Raynal, M.; Heun, S.; Pan, J.; Buchholz, H.; Braunstein, P.; De Cola, L. *Inorg. Chem.* **2013**, *52*, 10756.
(6) (a) Grushin, V. V.; Herron, N.; LeCloux, D. D.; Marshall, W. J.; Petrov, V. A.; Wang, Y. *Chem. Commun.* **2001**, 1494; (b) Coppo, P.; Plummer, E. A.; De Cola, L. *Chem. Commun.* **2004**, 1774; (c) Lowry, M. S.; Hudson, W. R.; Pascal Jr., R. A.; Bernhard, S. *J. Am. Chem. Soc.* **2004**, *126*, 14129; (d) Tamayo, A. B.; Garon, S.; Sajoto, T.; Djurovich, P. I.; Tsyba, I. M.; Bau, R.; Thompson, M. E. *Inorg. Chem.* **2005**, *44*, 8723; (e) Babudri, F.; Farinola, G. M.; Naso, F.; Ragni, R. *Chem. Commun.* **2007**, 1003; (f) Ladouceur, S.; Fortin, D.; Zysman-Colman, E. *Inorg. Chem.* **2011**, *50*, 11514; (g) Tordera, D.; Serrano-Pérez, J. J.; Pertegás, A.; Ortí, E.; Bolink, H. J.; Baranoff, E.; Nazeeruddin, M. K.; Frey, J. *Chem. Mater.* **2013**, *25*, 3391.
(7) (a) Takizawa, S.-y.; Nishida, J.-i.; Tsuzuki, T.; Tokito, S.; Yamashita, Y. *Inorg. Chem.* **2007**, *46*, 4308; (b) Xu, M.; Zhou, R.; Wang, G.; Xiao, Q.; Du, W.; Che, G. *Inorg. Chim. Acta* **2008**, *361*, 2407; (c) Sykes, D.; Tidmarsh, I. S.; Barbieri, A.; Sazanovich, I. V.; Weinstein, J. A.; Ward, M. D. *Inorg. Chem.* **2011**, *50*, 11323.
(8) (a) Tordera, D.; Bünzli, A. M.; Pertegás, A.; Junquera-Hernández, J. M.; Constable, E. C.; Zampese, J. A.; Housecroft, C. E.; Ortí, E.; Bolink, H. J. *Chem. Eur. J.* **2013**, *19*, 8597; (b) Constable, E. C.; Ertl, C. D.; Housecroft, C. E.; Zampese, J. A. *Dalton Trans.* **2014**, *43*, 5343.
(9) (a) Lee, S. J.; Park, K.-M.; Yang, K.; Kang, Y. *Inorg. Chem.* **2008**, *48*, 1030; (b) Yang, C.-H.; Mauro, M.; Polo, F.; Watanabe, S.; Muenster, I.; Fröhlich, R.; De Cola, L. *Chem. Mater.* **2012**, *24*, 3684; (c) Kessler, F.; Watanabe, Y.; Sasabe, H.; Katagiri, H.; Nazeeruddin, M. K.; Grätzel, M.; Kido, J. *J. Mater. Chem. C* **2013**, *1*, 1070; (d) Chang, C. H.; Wu, Z. J.; Chiu, C. H.; Liang, Y. H.; Tsai, Y. S.; Liao, J. L.; Chi, Y.; Hsieh, H. Y.; Kuo, T. Y.; Lee, G. H.; Pan, H. A.; Chou, P. T.; Lin, J. S.; Tseng, M. R. *ACS Appl. Mater. Interfaces* **2013**, *5*, 7341; (e) Frey, J.; Curchod, B. F. E.; Scopelliti, R.; Tavernelli, I.; Rothlisberger, U.; Nazeeruddin, M. K.; Baranoff, E. *Dalton Trans.* **2014**, *43*, 5667; (f) Evariste, S.; Sandroni, M.; Rees, T. W.; Roldan-Carmona, C.; Gil-Escrig, L.; Bolink, H. J.; Baranoff, E.; Zysman-Colman, E. *J. Mater. Chem. C* **2014**, *2*, 5793; (g) Lee, J.; Oh, H.; Kim, J.; Park, K.-M.; Yook, K. S.; Lee, J. Y.; Kang, Y. *J. Mater. Chem. C* **2014**, *2*, 6040.

(10) (a) Recent reviews: Jackson, D. A.; Mabury, S. A. *Environ. Toxicol. Chem.* **2009**, *28*, 1866; (b) Altomonte, S.; Zanda, M. *J. Fluorine Chem.* **2012**, *143*, 57; (c) Savoie, P. R.; Welch, J. T. *Chem. Rev.* **2014**, *115*, 1130.
(11) (a) Damerius, R.; Leopold, D.; Schulze, W.; Seppelt, K. *Z. Anorg. Allg. Chem.* **1989**, *578*, 110; (b) Preugschat, D.; Thrasher, J. S. *Z. Anorg. Allg. Chem.* **1996**, *622*, 1411; (c) Klauck, A.; Seppelt, K. *Angew. Chem. Int. Ed. Engl.* **1994**, *33*, 93; (d) Henkel, T.; Klauck, A.; Seppelt, K. *J. Organomet. Chem.* **1995**, *501*, 1; (e) Sitzmann, M. E.; Gilardi, R.; Butcher, R. J.; Koppes, W. M.; Stern, A. G.; Thrasher, J. S.; Trivedi, N. J.; Yang, Z.-Y. *Inorg. Chem.* **2000**, *39*, 843; (f) Winner, S. W.; Winter, R. W.; Smith, J. A.; Gard, G. L.; Hannah, N. A.; Rananavare, S. B.; Piknova, B.; Hall, S. B. *Mendeleev Commun.* **2006**, *16*, 182; (g) Frischmuth, A.; Unsinn, A.; Groll, K.; Stadtmuller, H.; Knochel, P. *Chem. Eur. J.* **2012**, *18*, 10234; (h) Joliton, A.; Carreira, E. M. *Org. Lett.* **2013**, *15*, 5147.
(12) (a) Sheppard, W. A. *J. Am. Chem. Soc.* **1962**, *84*, 3064; (b) Sheppard, W. A. *J. Am. Chem. Soc.* **1962**, *84*, 3072.
(13) Bowden, R. D.; Comina, P. J.; Greenhall, M. P.; Kariuki, B. M.; Loveday, A.; Philp, D. *Tetrahedron* **2000**, *56*, 3399.
(14) (a) De Angelis, F.; Fantacci, S.; Evans, N.; Klein, C.; Zakeeruddin, S. M.; Moser, J.-E.; Kalyanasundaram, K.; Bolink, H. J.; Gratzel, M.; Nazeeruddin, M. K. *Inorg. Chem.* **2007**, *46*, 5989; (b) Shavaleev, N. M.; Scopelliti, R.; Grätzel, M.; Nazeeruddin, M. K.; Pertegás, A.; Roldán-Carmona, C.; Tordera, D.; Bolink, H. J. *J. Mater. Chem. C* **2013**, *1*, 2241.
(15) Stille, J. K. *Angew. Chem. Int. Ed. Engl.* **1986**, *25*, 508.
(16) Harrowven, D. C.; Curran, D. P.; Kostiuk, S. L.; Wallis-Guy, I. L.; Whiting, S.; Stenning, K. J.; Tang, B.; Packard, E.; Nanson, L. *Chem. Commun.* **2010**, *46*, 6335.
(17) Wang, X.-j.; Tan, J.; Grozinger, K.; Betageri, R.; Kirrane, T.; Proudfoot, J. R. *Tetrahedron Lett.* **2000**, *41*, 5321.
(18) Correa, A.; Bolm, C. *Adv. Synth. Catal.* **2007**, *349*, 2673.
(19) (a) Nonoyama, M. *Bull. Chem. Soc. Jpn.* **1974**, *47*, 767; (b) Sprouse, S.; King, K. A.; Spellane, P. J.; Watts, R. J. *J. Am. Chem. Soc.* **1984**, *106*, 6647.
(20) Eaton, D. R.; Sheppard, W. A. *J. Am. Chem. Soc.* **1963**, *85*, 1310.
(21) (a) Li, L.; Brennessel, W. W.; Jones, W. D. *Organometallics* **2009**, *28*, 3492; (b) Davies, D. L.; Lowe, M. P.; Ryder, K. S.; Singh, K.; Singh, S. *Dalton Trans.* **2011**, *40*, 1028.
(22) He, L.; Duan, L.; Qiao, J.; Wang, R.; Wei, P.; Wang, L.; Qiu, Y. *Adv. Funct. Mater.* **2008**, *18*, 2123.
(23) (a) Jameson, D. L.; Blaho, J. K.; Kruger, K. T.; Goldsby, K. A. *Inorg. Chem.* **1989**, *28*, 4312; (b) Ayers, T.; Scott, S.; Goins, J.; Caylor, N.; Hathcock, D.; Slattery, S. J.; Jameson, D. L. *Inorg. Chim. Acta* **2000**, *307*, 7.
(24) Ladouceur, S.; Fortin, D.; Zysman-Colman, E. *Inorg. Chem.* **2010**, *49*, 5625. and references cited therein.
(25) (a) Parker, S. T.; Slinker, J. D.; Lowry, M. S.; Cox, M. P.; Bernhard, S.; Malliaras, G. G. *Chem. Mater.* **2005**, *17*, 3187; (b) Zysman-Colman, E.; Slinker, J. D.; Parker, J. B.; Malliaras, G. G.; Bernhard, S. *Chem. Mater.* **2008**, *20*, 388; (c) van Reenen, S.; Matyba, P.; Dzwilewski, A.; Janssen, R. A. J.; Edman, L.; Kemerink, M. *Adv. Funct. Mater.* **2011**, *21*, 1795.
(26) Tordera, D.; Meier, S.; Lenes, M.; Costa, R. D.; Ortí, E.; Sarfert, W.; Bolink, H. J. *Adv. Mater.* **2012**, *24*, 897.

(27) (a) van Reenen, S.; Matyba, P.; Dzwilewski, A.; Janssen, R. A. J.; Edman, L.; Kemerink, M. *J. Am. Chem. Soc.* **2010**, *132*, 13776; (b) Lenes, M.; Garcia-Belmonte, G.; Tordera, D.; Pertegás, A.; Bisquert, J.; Bolink, H. J. *Adv. Funct. Mater.* **2011**, *21*, 1581.
(28) (a) Plummer, E. A.; van Dijken, A.; Hofstraat, J. W.; De Cola, L.; Brunner, K. *Adv. Funct. Mater.* **2005**, *15*, 281; (b) He, L.; Duan, L.; Qiao, J.; Zhang, D.; Dong, G.; Wang, L.; Qiu, Y. *Org. Electron.* **2009**, *10*, 152; (c) He, L.; Duan, L.; Qiao, J.; Zhang, D.; Wang, L.; Qiu, Y. *Org. Electron.* **2010**, *11*, 1185; (d) Yun, S.-J.; Seo, H.-J.; Song, M.; Jin, S.-H.; Kim, Y. I. *Bull. Korean Chem. Soc.* **2012**, *33*, 3645.
(29) Lee, J.; Chopra, N.; Eom, S.-H.; Zheng, Y.; Xue, J.; So, F.; Shi, J. *Appl. Phys. Lett.* **2008**, *93*, 123306.
(30) Sasabe, H.; Kido, J. *Chem. Mater.* **2011**, *23*, 621.
(31) (a) Lo, S. C.; Anthopoulos, T. D.; Namdas, E. B.; Burn, P. L.; Samuel, I. D. W. *Adv. Mater.* **2005**, *17*, 1945; (b) Bolink, H. J.; Cappelli, L.; Cheylan, S.; Coronado, E.; Costa, R. D.; Lardies, N.; Nazeeruddin, M. K.; Orti, E. *J. Mater. Chem.* **2007**, *17*, 5032; (c) Kawamura, Y.; Brooks, J.; Brown, J. J.; Sasabe, H.; Adachi, C. *Phys. Rev. Lett.* **2006**, *96*, 017404.

TOC graphic.

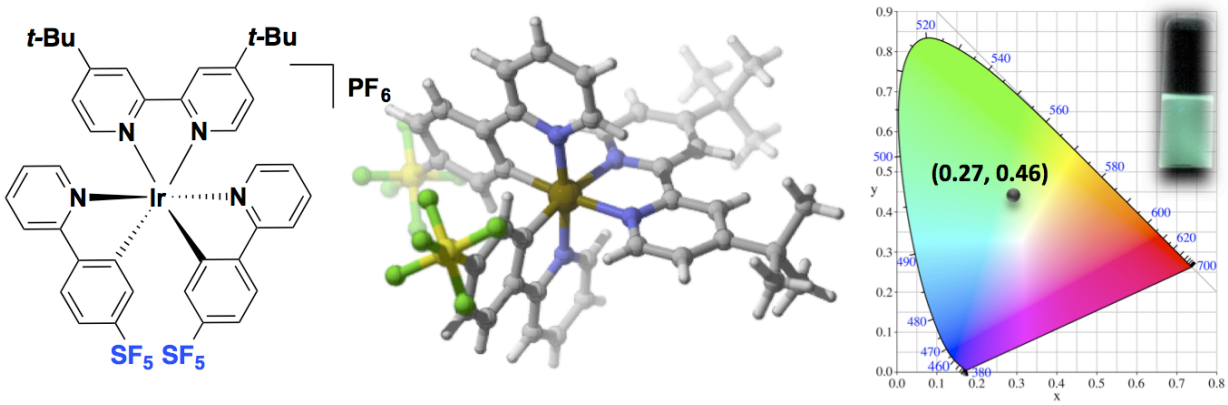

Synopsis

The first examples of iridium complexes bearing SF_5-functionalized cyclometalating ligands are reported. The SF_5 group promotes a large blue-shift in the emission spectrum compared to the non-substituted and fluoro- or trifluoromethyl-substituted analogues, with the family of complexes emitting brightly from 493-519 nm. LEEC devices did not work owing to the irreversible electrochemistry but green to yellow-green emitting OLEDs could be fabricated.